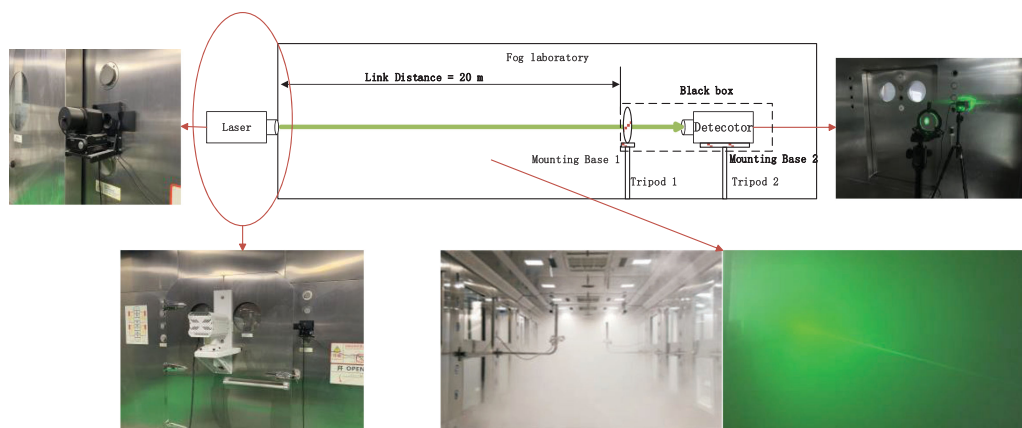


The Link Attenuation Model Based on Monte Carlo Simulation for Laser Transmission in Fog Channel

Volume 12, Number 4, August 2020

Siqi Hu
Huijie Liu
Lingfeng Zhao
Xiaolong Bian



DOI: 10.1109/JPHOT.2020.3006853

The Link Attenuation Model Based on Monte Carlo Simulation for Laser Transmission in Fog Channel

Siqi Hu ^{1,2}, Huijie Liu,^{1,2} Lingfeng Zhao,^{1,2} and Xiaolong Bian^{1,2}

¹Innovation Academy for Microsatellites of CAS, Shanghai 201203, China

²Shanghai Engineering Center for Microsatellites, Shanghai 201203, China

DOI:10.1109/JPHOT.2020.3006853

This work is licensed under a Creative Commons Attribution 4.0 License. For more information, see <https://creativecommons.org/licenses/by/4.0/>

Manuscript received April 3, 2020; revised June 2, 2020; accepted June 29, 2020. Date of publication July 3, 2020; date of current version July 14, 2020. Corresponding author: Siqi Hu. (email: siqi.hu@outlook.com).

Abstract: Free space optical (FSO) systems were usually designed according to the link budget analysis. However, the previous link attenuation estimations for fog channel were not precise. The link budget would be distorted, and resulting in the robustness degeneration of FSO system. Therefore, it is necessary to establish an accurate link attenuation model of fog channel. The previous models were mainly adopted by the Beer-Lambert law, or by classical Monte Carlo simulation combined with the fog drop size distribution. Unfortunately, the estimation deviation was eventually not fall within the acceptable range for FSO link budget analysis. We established a link attenuation model based on Monte Carlo simulation and Kim formula. Our model took the influence of multiple scattering and receiving parameters into consideration, and without the measurement of the fog drop size distribution and scattering cross-sections. The fog experiment was set up to verify the analysis results. And the experiment results revealed that the estimation deviation RMSE (root mean square error) < 1 , which validated the accuracy of link attenuation model. The link attenuation model can be used to strengthen the link budget analysis of FSO system and guide the parameter design of future FSO communication system under fog channel.

Index Terms: Link attenuation model, fog channel, monte carlo simulation, laser transmission, receiving parameters.

1. Introduction

With the development of high data rate optical communication systems in atmospheric transmission channels, the attenuation problem brought by visibility-limiting weather has hampered the free space optical communication systems [1]. One of the challenges of free-space optical communications is its susceptibility to attenuation by fog [2]. Especially in many military and civilian applications, the transmittance of laser beam in fog is a very important process [3]. FSO systems were usually designed according to the link budget analysis. However, The link margin is usually not abundant for satellite-to-earth laser communication due to the limited power and weight in satellite. According to the link budget analysis for optical links between ground station and OICETS(Optical Inter-orbit Communications Engineering Test Satellite), the uplink and downlink margin was 9.5 dB and 16.9 dB without considering the attenuation brought by fog, respectively [4]. In order to

guarantee the robustness of the FSO communication system, the link budget should be analyzed precisely. Therefore, it is necessary to establish an accurate link attenuation model of fog channel.

In the telecommunications industry, the Beer-Lambert law was typically developed to quantify the relationship between visibility and optical attenuation [1], [5]–[7]. The advantage of this method is the convenient in visibility measurement and simple calculation. However, this method has two disadvantages: Firstly, this method is limited to single scattering scenes with small attenuation length L_{att} ($L_{att} = \sigma \times L$, L is the link distance, σ is the attenuation coefficient) [8]; Secondly, the influence of receiver parameters is not considered. For small field-of-view and small aperture situations, the estimation has few deviations since the multiple scattering signal has been blocked by the receiver. However, this method would lead to large deviations for large field-of-view and large aperture situations. Three empirical formulas were used to predict the link attenuation in paper [9], and the experimental data was more significant than the empirical formulas predicted data. This is because the effects of receiving parameters and multiple scattering process are not taken into account, and resulting in the RMSE greater than 20 for all the empirical models.

The laser signal would suffered from multiple scattering during dense fog transmission, which needs to be took into consideration for link attenuation. The the multiple scattering can be regarded as a statistical result of random collisions between a large number of photons and scattered particles. Monte Carlo simulation is a very effective method to solve the problem of random distribution for laser transmission. However, there are two problems using classical Monte Carlo model to estimate the link attenuation in fog channel: Firstly, some papers used the fog drop size distribution and scattering cross-sections to calculate attenuation coefficient [8], [10], [11], but neither the fog drop size distribution nor scattering cross-sections of channel can be measured easily in practice, so this simulation method is not highly practical. Secondly, the influence of receiving parameters on link attenuation has not been analyzed which made the estimation deviations were eventually not fall within the acceptable range for link budget analysis [8], [10]–[13].

The multiple scattering process will cause the spot space to expand, the divergence angle to diffuse and the time domain to expand for the pulse signal. Different receiving parameters, such as receiving aperture and receiving field-of-view, will cause different link attenuation [14]. In a real communication scenario, the visibility information of fog is easily obtained from commercial visibility meters. Therefore, we established the relationship between visibility and attenuation coefficient based on Kim formula [1], and took the receiving parameters into consideration in the link attenuation model. The purpose of this paper is to establish an accurate link attenuation model of laser transmission in fog channel. The link attenuation model can be used to strengthen the link budget analysis and guide the parameters design of FSO communication system.

The content of this paper was arranged as follows. In Section 2, we established the link attenuation model for laser transmission in fog channel based on Monte Carlo simulation and Kim formula. In section 3, the influence of receiving aperture and receiving field-of-view on link attenuation were simulated and analyzed. In section 4, the experimental analysis for fog transmission with different receiving parameters was carried out to verify the influence of receiving parameters and test the accuracy of the link attenuation model.

2. The Link Attenuation Model in Fog Channel

Monte Carlo simulation can be used to calculate multiple laser scattering in random distribution, and is one of the commonly used numerical methods in laser transmission research [15]–[17]. The characteristics of laser signal through fog transmission are simulated by Monte Carlo method, which uses statistical method to describe the transmission law of photon, including the probability distribution of photon motion between two scattering points and the probability distribution of divergence angle. In Monte Carlo simulation, light is considered as a group of virtual photons or photon packets, and their propagation paths are generated to obtain accuracy results. The Monte Carlo method simulates the trajectories of a large number of emitted photons and obtains the transmission process and energy distribution of laser pulses [18]–[20].

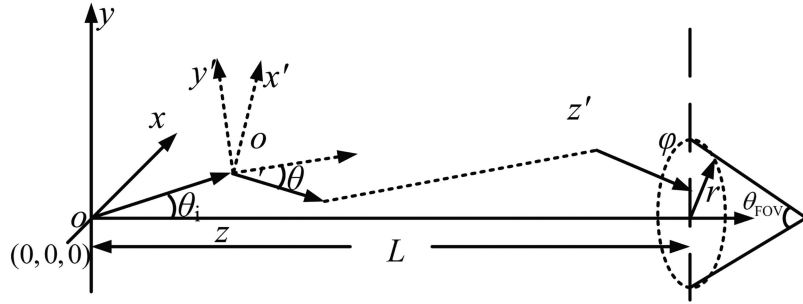


Fig. 1. The tracking process of Monte Carlo simulation.

The tracking process of Monte Carlo simulation is shown in Fig. 1. The laser emission position is determined as the origin, and the global coordinate system o - xyz is established with the laser transmission direction along z -axis. The initialization parameters include initial energy $E(0)$, initial position (x, y, z) and transmission direction (μ_x, μ_y, μ_z) of photon packet, where μ_x, μ_y, μ_z represent the cosine of photon transmission direction between X -axis, Y -axis and Z -axis respectively. The energy is sampled according to the gaussian distribution $n(0, \delta^2)$, where $n(u, \delta^2)$ is the gaussian distribution of mean μ and standard deviation δ . Each photon packet propagates along the transmission direction $\vec{r}_0 = (\mu_x, \mu_y, \mu_z)$, arrives at scatter point when transmitted to distance l_R (random step length). Random step length l_R is calculated by Eq. (1),

$$l_R = -\ln(\chi_R)/\sigma \quad (1)$$

Where χ_R is a random number satisfying uniform distribution $\mu(0, 1)$, and σ is the attenuation coefficient. σ can be calculated by the fog drop size distribution and scattering cross-sections [21], [22]. However, these parameters are not easy to be obtained at any given time, making it unpractical to determine the attenuation coefficient by using fog drop size distribution and scattering cross-sections. A more pragmatic approach relies merely on visibility - Kim formula is derived [1]. The relation between attenuation coefficient σ and visibility V is calculated by Eq. (2),

$$\sigma = \frac{3.91}{V} \left(\frac{\lambda}{550 \text{ nm}} \right)^{-q} \quad (2)$$

where the λ is the wavelength of laser. q is determined by the size of scattered particles, and is dependent on visibility, as shown in Eq. (3). After scattering, energy loss is calculated according to Eq. (4),

$$q = \begin{cases} 1.6, & V > 50 \text{ km} \\ 1.3, & 6 \text{ km} < V \leq 50 \text{ km} \\ 0.16V + 0.34, & 1 \text{ km} < V \leq 6 \text{ km} \\ V - 0.5, & 0.5 \text{ km} < V \leq 1 \text{ km} \\ 0, & V \leq 0.5 \text{ km} \end{cases} \quad (3)$$

$$E(L)_{post} = \omega E(L)_{pre} \quad (4)$$

where $E(L)_{pre}$ and $E(L)_{post}$ are the photon package energy before and after scattering at distance L , respectively. ω is the albedo ratio. Previous studies have proved that the scattering in fog belongs to molecular scattering, the absorption coefficient can be ignored, and the attenuation coefficient is approximately equal to the scattering coefficient, so the albedo ratio ω is set to 1 [17], [23]. The scattering angle θ and azimuthal angle ϕ are calculated according to the Henyey-Greenstein function, as shown in Eqs(5)[24]. After scattering process, the transmission direction of photon

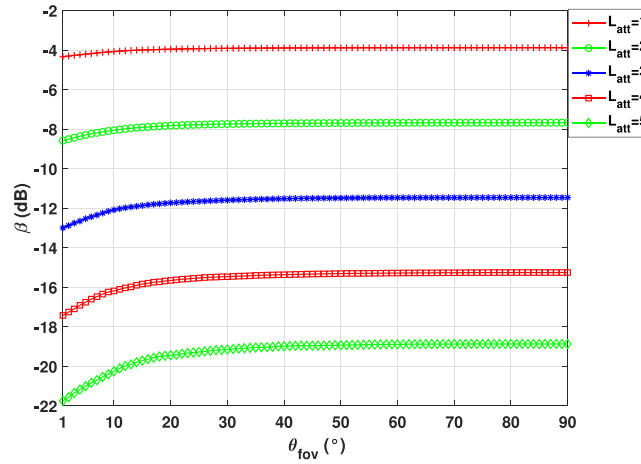


Fig. 2. The influence of the receiving FOV for the link attenuation ($D = 50$ mm).

packet will be updated to (μ'_x, μ'_y, μ'_z) according to Eq. (6).

$$\begin{cases} \theta = \arccos\left(\frac{1}{2g}\left(1 + g^2 - \left(\frac{1-g^2}{1+g-2gx_r}\right)^2\right)\right) \\ \varphi = 2\pi\chi_r \end{cases} \quad (5)$$

$$\begin{bmatrix} \mu'_x \\ \mu'_y \\ \mu'_z \end{bmatrix} = \begin{bmatrix} \mu_x\mu'_z\sqrt{1-\mu_z^2} - \mu_y/\sqrt{1-\mu_z^2} & \mu_x \\ \mu_y\mu'_z\sqrt{1-\mu_z^2} & \mu_x/\sqrt{1-\mu_z^2} & \mu_y \\ -\sqrt{1-\mu_z^2} & 0 & \mu_z \end{bmatrix} \begin{bmatrix} \sin(\theta)\cos(\varphi) \\ \sin(\theta)\sin(\varphi) \\ \cos(\theta) \end{bmatrix} \quad (6)$$

Let (l_x, l_y, l_z) represent the location of receiver system, R denotes the receiver radius and θ_{fov} is the field-of-view. When the photon packet arrived at the receiving plane (z equals to link distance), the energy of photon packet can be accumulated in receiver system when it satisfies Eq. (7). The link attenuation can be measured by counting the total energy of the photon packet entering the receiver.

$$\begin{cases} (x - l_x)^2 + (y - l_y)^2 \leq R^2 \\ \mu_z \geq \cos(\theta_{fov}) \end{cases} \quad (7)$$

3. The Influence of Receiving Parameters

Considering the influence of multiple scattering process, the laser spot will be expanded and the divergence angle will be diffused with the increment of attenuation length. Different receiving parameters, such as receiving aperture and the field-of-view, will cause different link attenuation. The analysis of the influence of receiving parameters for the link attenuation would be necessary. The simulation steps were established in section II, the initial divergence angle θ_t is set to 0.5 mrad and the wavelength is set to 532 nm. The link attenuation β is defined as Eq. (8), where P_t is the transmitted laser energy, and P_r is the received laser energy.

$$\beta = 10 \log_{10} \left(\frac{P_r}{P_t} \right) \quad (8)$$

In studying the influence of the receiving field-of-view for the link attenuation, we set the receiving diameter D to 50 mm, and simulated the link attenuation for different receiving field-of-view θ_{fov} and different attenuation length L_{att} . The result is shown in Fig. 2. In the examination of the influence of the receiving diameter for the link attenuation, we set the receiving field-of-view θ_{fov} to 15° and

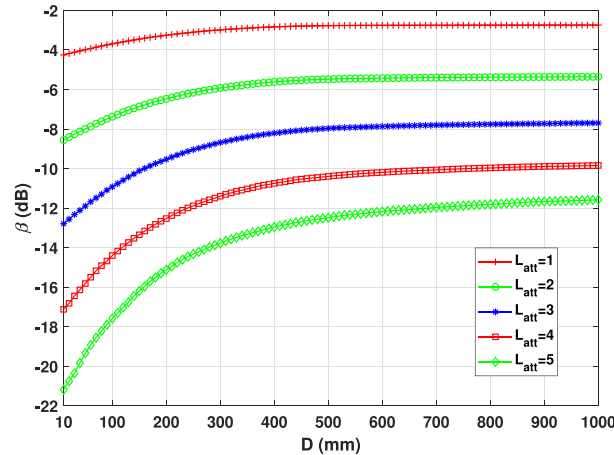


Fig. 3. The influence of the receiving diameter for the link attenuation ($\text{FOV} = 15^\circ$).

TABLE 1

The Link Attenuation Estimation by Empirical Formula Combined With the Beer-Lambert Law

L_{att}	1	2	3	4	5
$\beta(\text{dB})$	-4.34	-8.68	-13.03	-17.37	-21.71

simulate the link attenuation for different receiving diameter D and different attenuation length L_{att} . The outcome is demonstrated in Fig. 3.

According to the empirical formula combined with the Beer-Lambert law as shown in Eq. (9) [1], [7], the link attenuation estimation for $L_{att} = 1$ to $L_{att} = 5$ is shown in Table 1. For the situation when $\theta_{fov} = 1^\circ$ in Fig. 2 and $D = 10$ mm in Fig. 3, the link attenuation is consistent with the empirical formula combined with the Beer-Lambert law from attenuation length $L_{att} = 1$ to $L_{att} = 5$. Since the scattering photons has been blocked by narrow field-of-view or small aperture, the received laser energy is the part that did not experience scattering. These results reveal that the link attenuation estimation by empirical formula combined with the Beer-Lambert law is valid in narrow field-of-view or small aperture situation.

$$\beta = 10 \log_{10}(\exp(-L_{att})) \quad (9)$$

For the situation when $L_{att} = 1$ in Fig. 2 and Fig. 3, the simulation result tends to be a horizontal line. But for the situation when $L_{att} = 2$ to $L_{att} = 5$, the link attenuation will decrease with the increment of receiving FOV or receiving diameter. Ignoring the influence of receiving FOV or receiving diameter will result in huge simulation deviations. For example, in Fig. 2 when $L_{att} = 5$, the link attenuation for $\theta_{fov} = 23^\circ$ is -19.33 dB, but the link attenuation for $\theta_{fov} = 1^\circ$ is -21.75 dB, the deviation is 2.62 dB. And in Fig. 3 when $L_{att} = 5$, the link attenuation for $D = 670$ mm is -12.03 dB, but the link attenuation for $D = 10$ mm is -21.19 dB, the deviation is 9.16 dB. These results reveal that receiving parameters can not be ignored in link attenuation estimation, especially in high attenuation length situation.

With the increment of the receiving field-of-view or receiving diameter, more scattered photons enter the receiver and the link attenuation gradually decreases. When the receiving field-of-view or receiving diameter increases to a certain point, the link attenuation saturation does not decrease further. If we defined a saturation point for receiving field-of-view S_{fov} and receiving diameter S_d which can make receiver receive 90% scattered light energy as shown in Eq. (10) and Eq. (11), the received saturation points at different attenuation lengths can be obtained as shown in the Table 2. It shows that S_{fov} and S_d increase with the attenuation length. This result reveals that increasing the receiving field-of-view or receiving diameter improves the robustness of free space

TABLE 2
Saturation Point for Receiving Field-of-View and Receiving Diameter

L_{att}	1	2	3	4	5
$S_{fov} (^{\circ})$	1	8	15	18	23
S_d (mm)	220	330	420	540	670

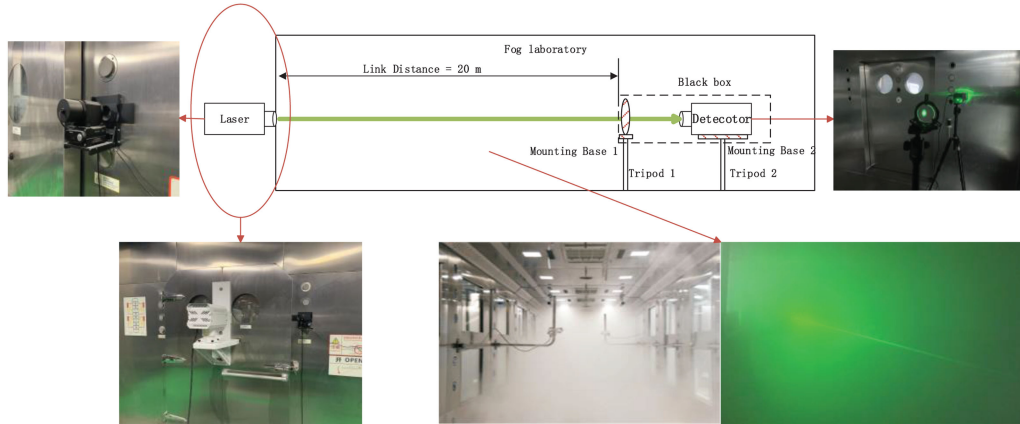


Fig. 4. Schematic diagram of fog experimental testing.

laser communication system for dense fog channel.

$$\beta_{fov}(S_{fov}) = 0.9 \times \beta_{fov}(90^{\circ}) \quad (10)$$

$$\beta_D(S_d) = 0.9 \times \beta_D(1000) \quad (11)$$

4. Experimental Testing

4.1 Experimental Scheme

A fog experiment is designed to verify the effect of receiving parameters on link loss and the accuracy of the link attenuation model. The visibility in the fog laboratory can be adjusted from 1 m to 1 km. The experimental space is 3 m \times 3 m \times 22 m, which leads the experimental attenuation length L_{att} can be varied from 0.08 (20 m \times 0.004/m) to 78.2 (20 m \times 3.91/m) according to Eq. (2) and Eq. (3).

The schematic diagram of the experiment is shown in Fig. 4. The laser was installed outside the laboratory chamber and transmitted laser to the laboratory chamber through a small hole. The receiver consisted of a convex lens and a detector. The tripod is used to adjust the height of detector and lens, in order to keep all the optical link in the same height. The lens and detector are shaded by black box. The receiving parameters can be adjusted according to the lens and distance between lens and detector. The link distance L is fixed to 20 m. Visibility in the chamber can be controlled at the external operating terminal of the laboratory, as shown in Fig. 5. The controllable stable time is 10 minutes and the visibility control deviation is less than 1 m.

In order to analyze the influence of receiving parameters for the link attenuation, we set receiving diameter D to 50 mm, and three different field-of-view ($\theta_{fov} = 1^{\circ}$, $\theta_{fov} = 15^{\circ}$, and $\theta_{fov} = 30^{\circ}$) were tested for the influence brought by receiving field-of-view experiment. And we fixed receiving field-of-view θ_{fov} to 15° , and three different receiving diameter ($D = 10$ mm, $D = 50$ mm, and $D = 100$ mm) were tested for the influence brought by receiving diameter experiment. The parameters of receiver are shown in the Table 3 and the parameters of transmitter are shown in the Table 4.



Fig. 5. Operation terminal.

TABLE 3
Receiver Parameters

Wavelength range	0.19 ~ 15 μ m
Beam Diameter	8.5 mm
Maximum average power density	1.5kW/cm ²
Equivalent noise power	10 μ W
Linearity	\pm 0.5%
Power range	10 μ W ~ 5W
Uncertainty (k = 2)	\pm 2%
Response time (0 ~ 90%)	< 1s
Receiving field-of-view θ_{fov} (°)	1, 15, 30
Receiving diameter D (mm)	10, 50, 100

TABLE 4
Transmitter Parameters

Wavelength	532 \pm 1nm
Operating mode	CW
Output power	1 W
Beam divergence	0.5mrad
Beam diameter at the aperture	2 mm
M^2 factor	1.2
Power stability	< 1%

4.2 Experimental Results

According to the Eq. (2), the visibility was adjusted from 8 m to 78 m, this range of visibility is correspond to attenuation length L_{att} varying from 1 to 10 ($L_{att} = \sigma \times L$, $L = 20$ m). The comparison between experimental results and simulation results for different θ_{fov} and D were shown in Fig. 6 and Fig. 7, respectively. From the experimental results, we can get three conclusions as follows:

1) For small field-of-view and small aperture situations as shown with the red line in Fig. 6 and Fig. 7, the link attenuation is consistent with the empirical formula combined with the Beer-Lambert law. Therefore, for small field-of-view and small aperture situations, the empirical formula is still applicable.

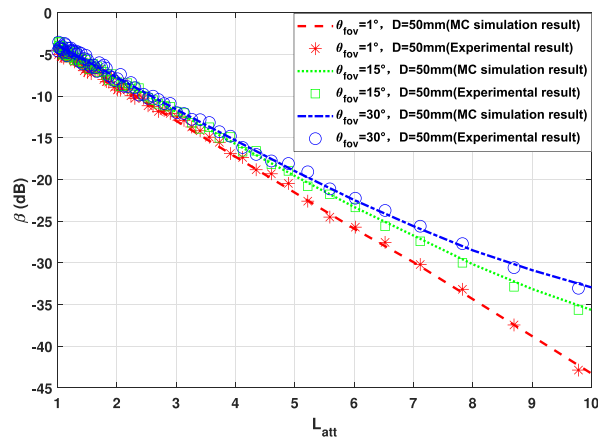


Fig. 6. Comparison between experimental results and simulation results for different θ_{fov} .

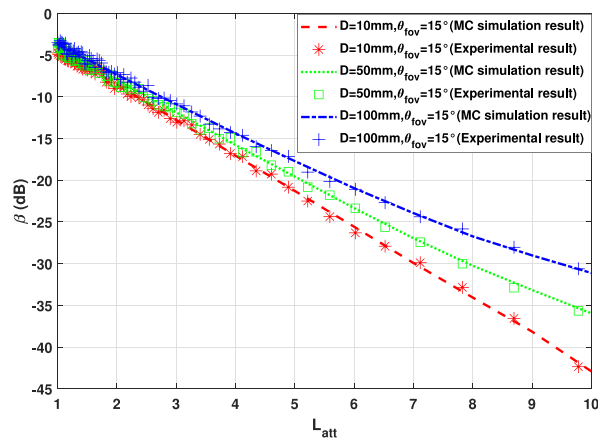


Fig. 7. Comparison between experimental results and simulation results for different D .

2) For low attenuation length, the receiving field-of-view and receiving aperture have little effect on link attenuation. With the increment of attenuation length, the link attenuation of large field-of-view and large aperture is significantly smaller than that of small field-of-view and small aperture. The influence of receiving parameters on link attenuation increases with the rise of attenuation length. The experimental results are consistent with the simulation analysis in section 3.

3) The experimental data was compared with the simulation data, the root mean square error (RMSE) was used to evaluate the accuracy of the link attenuation model. The RMSE was calculated according to Eq. (12),

$$RMSE = \sqrt{\frac{\sum_{i=1}^n (\beta_{ex,i}) - \beta_{mc,i})^2}{n}} \quad (12)$$

$\beta_{mc,i}$ is simulated specific link attenuation by link attenuation model, $\beta_{ex,i}$ is experimental measured link attenuation data, and n represents the total number of observations in Fig. 6 and Fig. 7. The RMSE between simulation results and experimental results for different receiving parameters were shown in the Table 5. It can be seen from the table that the RMSE of the link attenuation model for all the parameters were less than 1. This result reveals that the link attenuation model is accurate.

TABLE 5
The RMSE Between Simulation Results and Experimental Results

Receiving parameters	$\theta_{fov} = 1^\circ$ $D = 50mm$	$\theta_{fov} = 15^\circ$ $D = 50mm$	$\theta_{fov} = 30^\circ$ $D = 50mm$	$\theta_{fov} = 15^\circ$ $D = 10mm$	$\theta_{fov} = 15^\circ$ $D = 100mm$
RMSE	0.732	0.783	0.694	0.829	0.682

5. Conclusion

We established a link attenuation model based on Monte Carlo simulation and Kim formula. It took the influence of multiple scattering and receiving parameters into consideration, and without the measurement of the fog drop size distribution and scattering cross-sections. The results of simulation and experiment validated that the link attenuation is consistent with the empirical formula combined with the Beer-Lambert law for small field-of-view, small aperture situations and low attenuation length situations. But the estimation deviation of classical methods increased with the increment of field-of-view and aperture or attenuation length, which made them invalid to estimate the link attenuation of fog channel. However, our model maintained the estimation accuracy since the deviation $RMSE < 1$ for different receiving parameters situations during the fog experiment.

This result revealed that the link attenuation model can estimate the attenuation brought by fog channel precisely. And it can be used to strengthen the link budget analysis of FSO system and guide the parameter design of future FSO communication system under fog channel.

Acknowledgment

The authors wish to thank the anonymous reviewers for their valuable suggestions.

References

- [1] I. I. Kim, B. Mearthur, and E. J. Korevaar, "Comparison of laser beam propagation at 785 nm and 1550 nm fog and haze for optical wireless communications," *Proc. SPIE*, vol. 4214, no. 2, pp. 26–37, 2001.
- [2] K. W. Fischer*, M. R. Witiw, J. A. Baars+, and T. R. Oke, "Atmospheric laser communication," *Bull. Amer. Meteorological Soc.*, vol. 85, no. 5, pp. 725–732, 2004.
- [3] F. X. Kneizys, S. A. Clough, and E. P. Shettle, "Atmospheric attenuation of laser radiation," vol. 12, no. 3, pp. 346–348, 1970.
- [4] M. Toyoshima *et al.*, "Ground-to-satellite laser communication experiments," *IEEE Aerosp. Electron. Syst. Mag.*, vol. 23, no. 8, pp. 10–18, Aug. 2008.
- [5] P. W. Kruse, L. D. Mcglauchlin, and R. B. Mcquistan, *Elem. of Infr. Tech.: Gene., Transmi. and Dete.*. Amsterdam, The Netherlands: Elsevier, 1962.
- [6] A. Naboulsi and Maher, "Fog attenuation prediction for optical and infrared waves," *Opt. Eng.*, vol. 43, no. 2, pp. 319–329, 2004.
- [7] M. Gebhart, E. Leitgeb, S. S. Muhammad, B. Flecker, and H. Sizun, "Measurement of light attenuation in dense fog conditions for fso applications," *Proc. SPIE - Int. Soc. Opt. Eng.*, 2005, vol. 5891, pp. 175–186, doi: [10.1117/12.614830](https://doi.org/10.1117/12.614830).
- [8] H. X. Wang, C. Sun, Y. Z. Zhu, H. H. Sun, and P. S. Li, "Monte Carlo simulation of laser attenuation characteristics in fog," *Proc. SPIE - Int. Soc. Opt. Eng.*, 2011, vol. 8192, doi: [10.1117/12.899292](https://doi.org/10.1117/12.899292).
- [9] Khan and S. Muhammad, "Further results on fog modeling for terrestrial free-space optical links," *Opt. Eng.*, vol. 51, no. 3, 2012, Art. no. 031207.
- [10] B. Wang, G. Tong, and J. Lin, "Monte Carlo simulation of laser beam scattering by water droplets," in *Proc. Int. Symp. Photoelectronic Detection Imag.: Laser Sens. Imag. Appl.*, vol. 8905, 2013, pp. 726–733.
- [11] Y. Wei, Z. Wu, and W. Tao, "Research on the effects of offing fog on millimeter wave propagation," *Proc. SPIE - Int. Soc. Opt. Eng.*, vol. 9261, pp. 92 611B–92 611B–9, 2014.
- [12] F. Nadeem, M. S. Khan, and E. Leitgeb, "Optical wireless link availability estimation through monte carlo simulation," in *Proc. IEEE Int. Conf. Telecommun.*, 2011, doi: [10.4271/2011-01-0500](https://doi.org/10.4271/2011-01-0500).
- [13] T. J. P. Stillwell R A *et al.*, "Monte Carlo method for the analysis of laser safety for a high-powered lidar system under different atmospheric conditions," *J. Laser Appl.*, vol. 29, no. 2, 2017, Art. no. 022002.
- [14] J. S. L and W. L., "Monte Carlo modeling of light transport in tissues," *J. Comput. Methods Programs Biomedicine*, vol. 47, no. 2, pp. 131–146, 1995.
- [15] E. A. Bucher, "Computer simulation of light pulse propagation for communication through thick clouds," *Appl. Opt.*, vol. 12, no. 10, pp. 2391–400, 1973.
- [16] J. L. Bufton, L. O. Caudill, T. E. Mcgunigal, and K. R. Piech, "Skylab-earth laser-beacon experiment: Results and analysis," *J. Opt. Soc. Amer.*, vol. 69, no. 8, pp. 1180–1183, 1979.

- [17] G. N. Plass and G. W. Kattawar, "Monte Carlo calculations of light scattering from clouds," *Appl. Opt.*, vol. 7, no. 3, pp. 415–419, 1968, doi: [10.1364/AO.7.000415](https://doi.org/10.1364/AO.7.000415).
- [18] C. Gabriel, M. A. Khalighi, P. Leon, S. Bourennane, and V. Rigaud, "Monte-carlo-based channel characterization for underwater optical communication systems," *IEEE/OSA J. Opt. Commun. Netw.*, vol. 5, no. 1, pp. 1–12, Jan. 2013.
- [19] D. J. Bogucki, J. Piskozub, M. E. Carr, and G. D. Spiers, "Monte Carlo simulation of propagation of a short light beam through turbulent oceanic flow," *Opt. Express*, vol. 15, no. 21, pp. 13 988–96, 2007.
- [20] K. Yu and T. Iwai, "Hybrid Mie-MCML Monte Carlo simulation of light propagation in skin layers," in *Proc. Int. Conf. Opt. Part. Charact.*, 2014, pp. 923 206–923 206–4.
- [21] R. W. Redington, "Elements of infrared technology: Generation, transmission, and detection," *Solid-State Electron*, vol. 5, 1962.
- [22] F. G. Smith, "Atmospheric propagation of radiation," *Infrared and Electro-Optical Systems Handbook*, vol. 2, 1993.
- [23] P. M. Hesse and I. Schult, "Optical properties of aerosols and clouds: The software package opac," *Bull. Amer. Meteorological Soc.*, vol. 79, no. 5, pp. 831–844, 1998.
- [24] C. F. Bohren and D. R. Huffman, "Absorption and scattering of light by small particles," *J. Colloid Interface Sci.*, vol. 98, no. 1, pp. 290–291, 1998.